ACCSCIENCE PUBLISHING

Cancer Plus

PERSPECTIVE ARTCLE

Application of CRISPR–Cas9 technology in the treatment of chronic lymphocytic leukemia with *TP53* mutations

Aurelian Udrițioiu[1]*, Liviu Martin[1], Delia Nica-Badea[2], Adrian Victor Tetileanu[3], Manole Cojocaru[4], and Ioan-Ovidiu Gheorghe[2]

[1]Department of Molecular Biology, Titu Maiorescu University of Bucharest, Faculty of Medicine, Assistance General Care, Târgu-Jiu, Gorj, Romania

[2]Department of Hematology, Faculty of Medical Science and Behaviour, Constantin Brâncuși University, Târgu-Jiu, Gorj, Romania

[3]Department of Gynecology, Emergency County Hospital Targu Jiu, Targu Jiu, Romania

[4]Department of Physiology, Faculty of Medicine, Titu Maiorescu University of Bucharest, Romanian Academy of Scientists, Bucharest, Romania

Abstract

This Perspective explores the potential implementation of clustered regularly interspaced short palindromic repeats (CRISPR)–CRISPR-associated protein 9 (Cas9) technology for gene therapy targeting pathogenic mutations in human lymphocytes affected by chronic lymphocytic leukemia (CLL). Drawing on existing evidence and limited preliminary observations, we discuss how this approach may offer new opportunities for treating this genetically heterogeneous disease. It focuses on the application of CRISPR–Cas9-mediated targeted sequencing to systematically characterize the biological effects of monoallelic and biallelic *TP53* gene lesions, aiming to replace mutant *TP53* genes in CLL cells through this technology. CRISPR–Cas9 technology employs a specific enzyme guided by a designed guide RNA (gRNA) to a DNA target. The enzyme first introduces a cut at the target site, and following this cleavage event, it can further disrupt the *TP53* gene. The gRNA plays a crucial role by directing the Cas9 protein to the DNA sequence of interest. The gRNA consists of CRISPR RNA (crRNA) and trans-activating CRISPR RNA (tracrRNA) sequences, responsible for target recognition and Cas9 binding, respectively. Examination of the predicted secondary structure of the tracrRNA–crRNA duplex suggests that the features required for Cas9-catalyzed DNA cleavage at specific sites can be captured within a single chimeric RNA. Although the natural tracrRNA–crRNA mechanism operates efficiently, the use of a single RNA-guided Cas9 system is particularly attractive due to its potential for programmed DNA cleavage and genome editing. Importantly, Cas9 can bind and cleave a target sequence only if it is adjacent to a protospacer adjacent motif. Once the gRNA–Cas9 complex binds to the target DNA, Cas9 induces a double-strand break at the specified site. In conclusion, this paper proposes that CRISPR–Cas9 technology represents a potential genetic engineering tool for advancing the treatment of chronic lymphocytic leukemia with *TP53* mutations.

Keywords: CRISPR–Cas9; *TP53* gene; p53 isoforms; Single guide RNA; Homology-directed repair; Zinc-finger nuclease; Nuclease; Trans-activator RNA

***Corresponding authors:**
Aurelian Udrițioiu
(aurelian.udristioiu.@prof.utm.ro)

Citation: Udrițioiu A, Martin L, Nica-Badea D, *et al*. Application of CRISPR–Cas9 technology in the treatment of chronic lymphocytic leukemia with *TP53* mutations. *Cancer Plus*. 2025;7(4):16-25. doi: 10.36922/CP025310048

Received: July 31, 2025

Revised: September 9, 2025

Accepted: September 19, 2025

Published online: October 28, 2025

1. Introduction

The diagnosis, clinical staging, and therapeutic response evaluation of chronic lymphocytic leukemia (CLL) are based on the criteria recommended by the International Workshop on CLL. Patients underwent complete physical examinations for the diagnosis of B-cell CLL (B-CLL), presenting with symptoms such as persistent cough, night sweats, and retrosternal pain.

In addition, patients were assessed using ultrasound and computed tomography–positron emission tomography imaging, which revealed lymphadenopathy or splenomegaly, including an enlarged spleen characteristic of hematologic disease. The diagnosis of CLL was further supported by cytological examination of peripheral blood smears under microscopy, showing an absolute lymphocyte count >5,000/μL with <10% prolymphocytes in the differential blood count.

In CLL, flow cytometry confirmed that the presence of a clonal B-cell population expressing cluster of differentiation (CD) 5^+, $CD19^+$, $CD20^{+/-}$, and $CD23^+$ is usually sufficient to establish the diagnosis.[1] The CD38 receptor is considered positive if lymphocytes display stronger staining intensity than granulocytes in the sample, and its expression is also associated with ζ-chain-associated protein kinase 70, an adverse prognostic marker.[2] Giemsa staining of these cells revealed atypical morphologies, including irregular cytoplasm, degenerative vacuoles, and frequent multinucleation, suggesting profound mitotic defects (Figure 1).

Mutations in the *TP53* gene are common in human neoplasia. A single allele mutation can cause hereditary cancer susceptibility syndromes such as Li–Fraumeni syndrome. Variants of this gene encode distinct p53 protein isoforms, which may disrupt transcriptional activity. Notably, the mitotic index was significantly lower in CLL cells harboring biallelic ataxia-telangiectasia mutated (*ATM*) and *TP53* loss than in CLL cells without such genetic alterations.

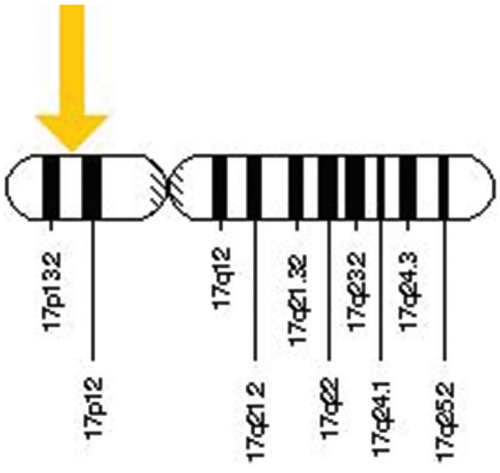

Figure 1. The *TP53* gene is located on the short (p) arm of chromosome 17, at position 13.1. More specifically, the *TP53* gene is located from base pair 7,668,402 to base pair 7,687,550 on chromosome 17. Adapted from Udristioiu *et al.*[31]

Approximately 80% of patients with 17p13 chromosomal deletion harbor mutations in the remaining *TP53* allele, resulting in loss of p53 protein function. Non-deletion mutations occur in approximately 4–5% of cases. While *TP53* mutations are generally associated with poor prognosis, not all mutations predict equivalent disruption of the p53 pathway. Moreover, a subset of patients with 17p13 deletion exhibit an indolent clinical course, suggesting that p53 function can sometimes be preserved.[3]

TP53 mutations are considered "multi-hit" if one of the following criteria is met: (i) The presence of two distinct *TP53* mutations; (ii) a single *TP53* mutation with a variant allele frequency >50%; or (iii) a single *TP53* mutation accompanied by 17p deletion on karyotyping. Multi-hit *TP53* mutations correlate strongly with high-risk disease features, complex karyotypes, and poor survival outcomes.[4] This Perspective aims to contextualize the potential role of CRISPR–Cas9–based gene editing in CLL, with a particular focus on TP53 mutations. By synthesizing existing evidence and incorporating limited real-world implementation insights, we discuss the feasibility of this approach and outline considerations for its practical applications.

2. Identification of p53 isoforms using enzyme-linked immunosorbent assay (ELISA)

In recent years, it has been discovered that the production of certain isoforms of the p53 protein, which exhibit increased stability in B lymphocytes, contributes to the process of carcinogenesis. This finding facilitated the identification of p53 protein isoforms using different methods, including immunohistochemistry and ELISA. Among these, ELISA is widely used as an initial screening method for detecting p53 isoforms generated by mutant *TP53* genes.

2.1. Principle of the ELISA

This assay is based on the principle of a sandwich ELISA. Each well of the microtiter plate is pre-coated with a specific capture antibody. When standards or samples are added, the target antigen—in this case, the p53 protein—binds to the capture antibody.

In this work, a specific kit for the human p53 protein (aa20–25) was used, employing a purified monoclonal

antibody (clone DO-1, isotype IgG2a). The PAb 240 antibody was also utilized for its specific binding to denatured p53 protein. Compatible sample types included both plasma and serum, which were processed using 96-well microplates.

2.2. ELISA protocol for detecting p53 isoforms in CLL samples

Reagents, samples, and standards are prepared according to the manufacturer's instructions. Human samples are used as described in the product leaflet. Sample types include cell culture supernatants, plasma, and serum, and assays are performed using 96-well microplates. A volume of 100 μL of standard or sample is then added to each well. For blood collected with ethylenediaminetetraacetic acid as an anticoagulant, lymphocytes are isolated and prepared for the assay. Plasma is collected using ethylenediaminetetraacetic acid or heparin-coated vacutainers and centrifuged at 4,500 rpm (approximately 280 × g) for 15 min. Following centrifugation, plasma is separated from red blood cells and fractionated into four distinct layers, with lymphocytes forming a visible "buffy coat." Using a pipette, 100 μL of the lymphocyte layer is carefully extracted (Figure 2).

2.3. Prognostic assessment

One of the most widely used prognostic scores in CLL is the CLL International Prognostic Index. This score integrates five independent prognostic factors: *TP53* deletion and/or mutation (collectively referred to as *TP53* dysfunction), immunoglobulin heavy chain variable region (*IGHV*) mutational status, serum β2-microglobulin, clinical stage, and patient age. Elevated levels of β2-microglobulin (≥5 mg/L) and lactate dehydrogenase (>250 U/L) are used to stratify patients into three prognostic risk groups, with corresponding 3-year survival rates of 63%, 83%, and 93%. Richter transformation occurs in 17% of patients in the high-risk group but in none of the patients in the low-risk group.[5]

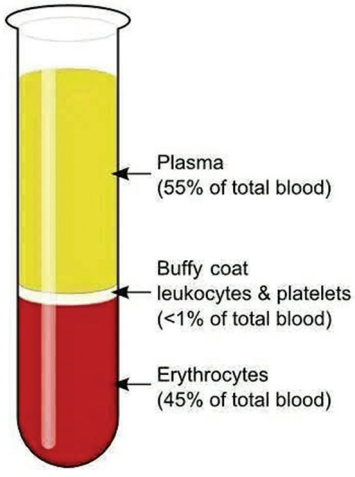

Figure 2. Plasma fractionated into four distinct fractions, overlaid on a leukocyte layer

3. Molecular biology and diagnostic advances of *TP53* in CLL

3.1. Structure of the normal *TP53* gene

A total of 12 human p53 protein isoforms are identified: p53α, p53β, p53γ, Δ40p53α, Δ40p53β, Δ40p53γ, Δ133p53α, Δ133p53β, Δ133p53γ, Δ160p53α, Δ160p53β, and Δ160p53γ. These isoforms are expressed in a tissue-dependent manner, and importantly, p53α is never expressed alone. Missense mutations affecting direct contact between the p53 protein and DNA can be retrieved from the International Agency for Research on Cancer database, specifically codons 239, 241, 248, 273, 275, 277, and 280.

In a previous study, the *TP53* gene chip was tested in collaboration with the International Agency for Research on Cancer partners. Missense mutations in structural p53 DNA-binding motifs were localized to the L2 and L3 loops, which interact with DNA in the minor groove (codons 164–194 and 237–250, respectively), or within the loop-sheet-helix motif, which interacts with DNA in the major groove (codons 119–135 and 272–287). These DNA-binding motifs are part of the DNA-binding domain (DBD; codons 102–292).[6]

All mutations included in the *TP53* database can be carefully analyzed and manually reviewed using Mutalyzer (https://mutalyzer.nl/). In solid tumors, *TP53* is mutated or deleted in approximately 50% of cases. In contrast, *TP53* aberrations are rare in leukemia, ranging from 5–10% at the time of diagnosis. Notably, hematopoietic stem cells (HSCs) carrying *TP53* missense mutations in the DBD demonstrate a competitive fitness advantage compared with HSCs harboring monoallelic *TP53* inactivation.[7]

Although *TP53*-mutant HSCs may promote self-renewal, they do not induce overt leukemic transformation, indicating that the presence of mutant *TP53* alone is insufficient to initiate leukemia. Additional selective pressures are required for clonal expansion, evolution, and transformation.[8] Importantly, *TP53* mutations are often missed at diagnosis using routine fluorescence *in situ* hybridization screening.[9]

In normal fluorescence in situ hybridization analysis, two red signals (for the *TP53* locus) and two green

signals (for the *ATM* locus) are observed. In CLL, genetic heterogeneity of susceptibility has been mapped to the most distal band on chromosome 17p13 (Figures 3 and 4).

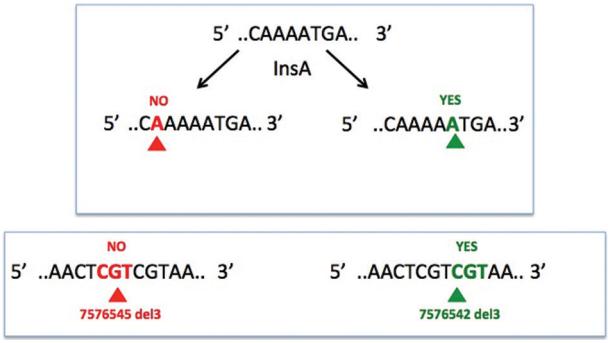

Figure 3. All mutations included in the *TP53* database can be carefully analyzed and manually reviewed using Mutalyzer (https://mutalyzer.nl/)[31]

3.2. Advanced diagnostic tools

For confirmatory diagnosis of CLL cases with p53 isoforms expressed in the nucleus and cytoplasm, next-generation sequencing (NGS) is essential. NGS can detect the full spectrum of mutations leading either to mutant p53 protein expression (e.g., missense mutations) or to complete loss of p53 expression (e.g., nonsense mutations, frameshifts, or splice-site alterations). This method provides high sensitivity across multiple sample types.

Modern molecular biology and bioinformatics tools—such as polymerase chain reaction, NGS, and karyotyping—are now indispensable for understanding the pathogenesis of hematologic malignancies. Pan-cancer NGS enables the detection of *TP53* variants, including single-nucleotide variants, monoallelic or biallelic copy number variants, insertions/deletions (indels), translocations, and gene fusions.

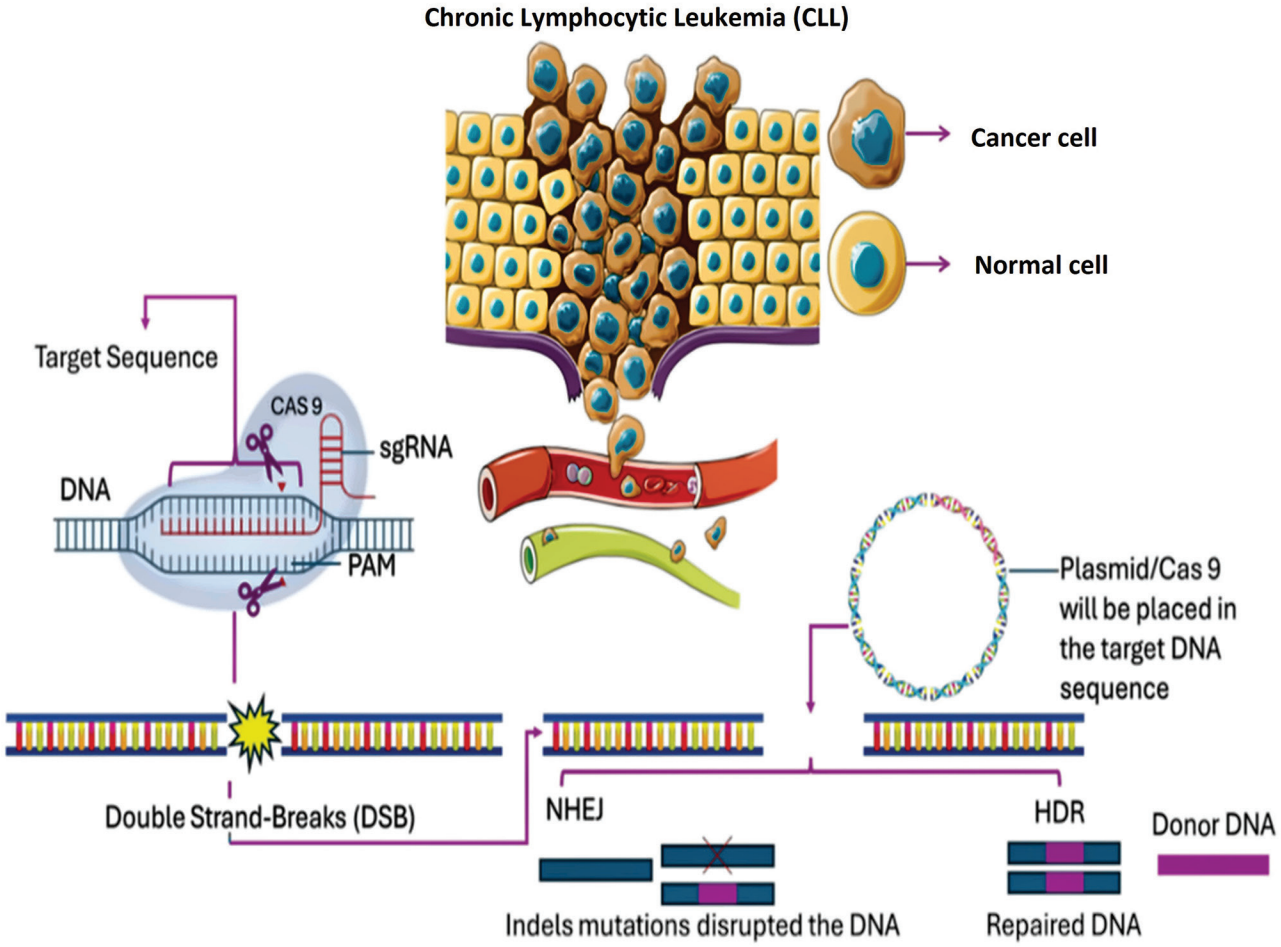

Figure 4. CRISPR–Cas9 gene editing
Abbreviations: AML: Acute myeloid leukemia; Cas9: Clustered regularly interspaced short palindromic repeats-associated protein 9; CRISPR: Clustered regularly interspaced short palindromic repeats; DSB: Double-strand break; HDR: Homology-directed repair; NHEJ: Non-homologous, end joining; sgRNA: Single guide RNA.

Missense mutations typically result in aberrant p53 protein expression with a dominant-negative effect, whereas null mutations (e.g., nonsense, splice-site, and frameshift mutations) lead to complete loss of protein expression. Both null and missense *TP53* mutations exert similar effects on survival outcomes. For this reason, *TP53* sequencing using NGS is recommended before treatment initiation in all patients enrolled in clinical trials, as outlined in the National Comprehensive Cancer Network Guidelines.[10]

Genomic DNA is often isolated from bone marrow using formalin-fixed, paraffin-embedded samples, which are the most commonly available materials for molecular testing. DNA extracted from lymphocytes in formalin-fixed, paraffin-embedded samples is usually fragmented (approximately 180 base pairs [bp]), requiring ≤20 ng of DNA input. Sensitivity can reach a 1% variant allele frequency by combining short-amplicon polymerase chain reaction with variant-enriched single-base extension chemistry—higher sensitivity than most conventional NGS assays.[11]

4. CRISPR–Cas9 technology for CLL treatment targeting mutant *TP53*

Clustered regularly interspaced short palindromic repeats (CRISPR)–CRISPR-associated protein (Cas)-9 technology can be delivered in several forms: Plasmid DNA encoding both Cas9 protein and single-guide RNA (sgRNA), CRISPR mRNA with sgRNA, or as a ribonucleoprotein (RNP) complex consisting of Cas9 protein bound to sgRNA. Alternative nucleases include smaller Cas9 variants or Cpf1 (Cas12a), which has gained popularity due to efficient transport and distinct protospacer adjacent motif (PAM) requirements.[12]

The CRISPR–Cas9 system is a versatile tool for introducing targeted mutations or insertions in genomic DNA. The system comprises a short non-coding guide RNA (gRNA) with two components: a CRISPR RNA (crRNA), which provides sequence specificity, and a trans-activating crRNA (tracrRNA), which binds Cas9. The gRNA directs Cas9 to the target genomic sequence, where Cas9 introduces a double-strand break (DSB).

Following DNA cleavage, repair is mediated by the cell's endogenous pathways. Non-homologous end joining often results in indels that can disrupt gene function, whereas homology-directed repair enables precise insertion or correction if a DNA repair template is provided. Despite improvements, homology-directed repair efficiency remains low in non-dividing cells, limiting therapeutic integration. Moreover, DSBs can lead to deleterious outcomes such as large deletions or chromosomal translocations.[13]

Caspase activation plays an important role downstream of CRISPR-induced apoptosis. Caspases cleave cytoskeletal proteins, nuclear pore components, the nuclear lamina, DNAse-inhibitory proteins, and poly(adenosine diphosphate-ribose)-polymerase, ultimately degrading chromatin and nuclear structure. Mitochondria contribute by activating procaspase-9 through adaptor proteins.[14]

4.1. Loading large DNA payloads into CRISPR systems

At its most basic level, CRISPR requires two components: A Cas nuclease and a gRNA. Together, they form an RNP complex that targets a 20-base protospacer adjacent to a PAM. PAM sequences vary depending on the Cas enzyme used. Once bound, Cas9 generates a precise blunt or staggered DSB. The gRNA spacer sequence is complementary to the protospacer, ensuring target specificity.

Recent advances in prime editing enable the insertion of larger DNA sequences without DSBs. GRAND editing, described by Zhang *et al*.,[15] uses pairs of prime editing gRNAs to insert up to approximately 1 kb of DNA. However, efficiency drops markedly when the insertion exceeds approximately 400 bp. Alternative approaches are being developed, such as preprint methods using dual prime editing gRNAs to improve long-fragment integration.[16]

4.2. *TP53* mutation landscape

Most *TP53* mutations are missense variants, although nonsense, splice-site, and frameshift mutations also occur, with the majority clustered within the DBD (exons 5–8). Six common mutation hotspots include R175H, Y220C, M237I, R248Q, R273H, and R282W. These mutations vary in their impact, ranging from complete loss of tumor suppressor function to partial loss or even gain-of-function activities.[17]

Optimizing reverse transfection of synthetic gRNAs into Cas9-expressing cell lines involves strict controls, continuous monitoring, and fine-tuning of delivery conditions. CRISPR screening strategies achieve stable gene editing through plasmid DNA integration while minimizing innate immune responses.[18,19]

4.3. Key components of CRISPR–Cas9 technology

Key components of the CRISPR–Cas9 technology include:

(i) gRNA: Laboratory-designed RNA that locates the target gene. Chimeric sgRNAs direct Cas9 to create DSBs near PAM sequences. Synthetic two-part gRNAs (separate crRNA and tracrRNA) are also used.

(ii) TracrRNA: Partners with crRNA to form the two-RNA structure that directs Cas9 to induce DSBs at the target site.

(iii) Positive and negative controls: CRISPR experiments employ TrueGuide crRNA positive controls and appropriate negative controls to validate editing efficiency and minimize off-target effects.[20]

4.4. The application of the CRISPR system in functional genomics of CLL

4.4.1. Future perspectives: CRISPR in CLL

The potential application of CRISPR technology in CLL follows models established in other hematologic disorders, such as β-thalassemia and sickle cell anemia—severe hereditary hemoglobinopathies, where CRISPR–Cas9 has been successfully used for gene replacement and correction. These advances highlight CRISPR as a promising tool for future targeted gene therapy in CLL. CRISPR systems are also used during assay development and as plate controls in screening experiments.[21-23]

4.4.2. Assessing gene editing efficiency

Following transfection with the CRISPR–Cas9 system, it is essential to evaluate gene editing efficiency by monitoring cleavage at control loci. The condition with the highest efficiency should then be selected for subsequent experiments. The GeneArt Genomic Cleavage Detection Kit provides a rapid, reliable method to measure CRISPR–Cas9 cleavage efficiency in pooled cell populations.[24]

Non-viral delivery platforms such as lipid nanoparticles, cell-penetrating peptides, DNA "nano-claws," and gold nanoparticles have been explored; however, efficient delivery remains a significant challenge in hematological malignancies.

Current approaches allow CRISPR–Cas9-mediated repair or replacement of mutant *TP53* genes at endogenous promoters, but they require prolonged cell culture and selection of corrected HSCs. Further progress in HSC growth and expansion is needed before clinical application.[25]

The detailed methodology for treating CLL using CRISPR–Cas9 technology targeting mutant *TP53* is described below:

(a) Tissue culture
Induced pluripotent stem (iPS) cells are cultured in Essential 8™ medium on vitronectin-coated plates under serum-free conditions, according to the manufacturer's recommendations. Cells are passaged using ReLeSR and supplemented with RevitaCell during passaging. The medium is replaced every 24 h.

(b) Media, supplements, and reagents
Gibco cell culture media is used for maintaining mammalian cells, ensuring reproducibility and consistency of experimental results.[26]

(c) Transfection
Transfection is performed using Lipofectamine™ reagents and Neon™ electroporation. Cleavage efficiency is assessed 72 h post-transfection with the GeneArt Genomic Cleavage Detection Kit.[27,28]
Hematopoietic stem cells are isolated from CLL patients, and Cas9 with sgRNAs are delivered as RNP complexes or plasmids. Successfully edited HSCs are evaluated and reintroduced into conditioned patients. This strategy is particularly suitable for hematologic disorders caused by single-gene mutations affecting myeloid and/or lymphoid lineages.

(d) Hematopoietic differentiation
Hematopoietic stem cells are the central drivers of hematopoiesis, producing both common myeloid progenitors and common lymphoid progenitors (CLPs). CLPs give rise to lymphocytes, whereas common myeloid progenitors generate mature myeloid cells via megakaryocyte–erythroid progenitors and granulocyte–monocyte progenitors.[29]
B-cell development begins in the bone marrow from pluripotent HSCs. Early progenitors express $CD34^+$, TdT^+, $CD19^+$, $CD79a^+$, $cyCD22^+$, HLA-DR^+, but are $CD10^-$ and $sIgM^-$. Precursor B cells are characterized by $CD34^+$, TdT^+, $CD45\text{^}dim^+$, $CD19^+$, $CD79a^+$, $cyCD22^+$, HLA-DR^+, $CD10\text{^}int^+$, $cyIgM^+$, and $sIgM^+$. As B cells mature, they progress from immature $CD10^+$ to naïve and finally to mature $CD10^-$ B cells, ultimately populating both bone marrow and peripheral blood (Figure 5).[30]

(e) Allogeneic hematopoietic cell transplantation
Currently, allogeneic hematopoietic cell transplantation remains the only potentially curative

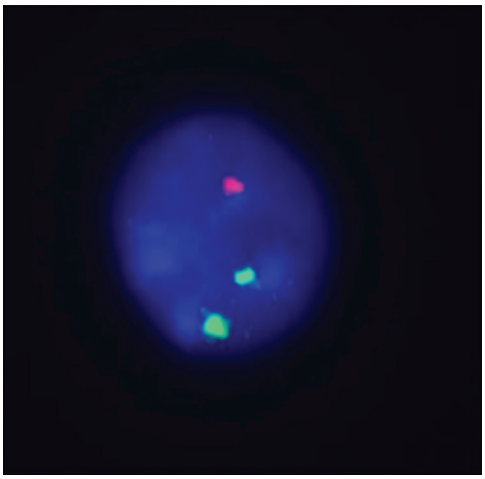

Figure 5. The image depicts the absence of a specific signal labeled with red fluorochrome (*TP53* locus) and the presence of two specific signals labeled with green fluorochrome (*ATM* locus), a pattern compatible with deletion of the *TP53* locus (generic image)

option for *TP53*-mutated CLL. HSCs appear as immature $CD34^+/CD38^-$ cells. Immunophenotypic testing should also evaluate CD45 isoforms (e.g., CD45RB, CD45RO, and CD45RA) in $CD34^+$ cells to distinguish malignant HSCs from malignant CLPs. *Ex vivo* HSC properties can be assessed by culturing cells in semi-solid media and quantifying their ability to form multilineage colony-forming units.

4.4.3. Sample preparation

For sample preparation, 2 mL of bone marrow aspirate is required, which is sufficient for analysis and can be stored at 4°C for up to 72 h. Samples obtained by flow cytometry should be accompanied by an unstained smear from the same sample during transport to the laboratory.

For sample processing, wash–stain–lyse methods are recommended, with washing as the preferred approach. Samples are diluted to obtain 10^5–10^6 cells per tube and aliquoted into 25–100 µL volumes. Care must be taken during centrifugation to avoid destroying lymphoblasts.

Labeling is a thermodynamic process between antibodies and antigens and should be performed for no longer than 15–20 min, at room temperature and in the

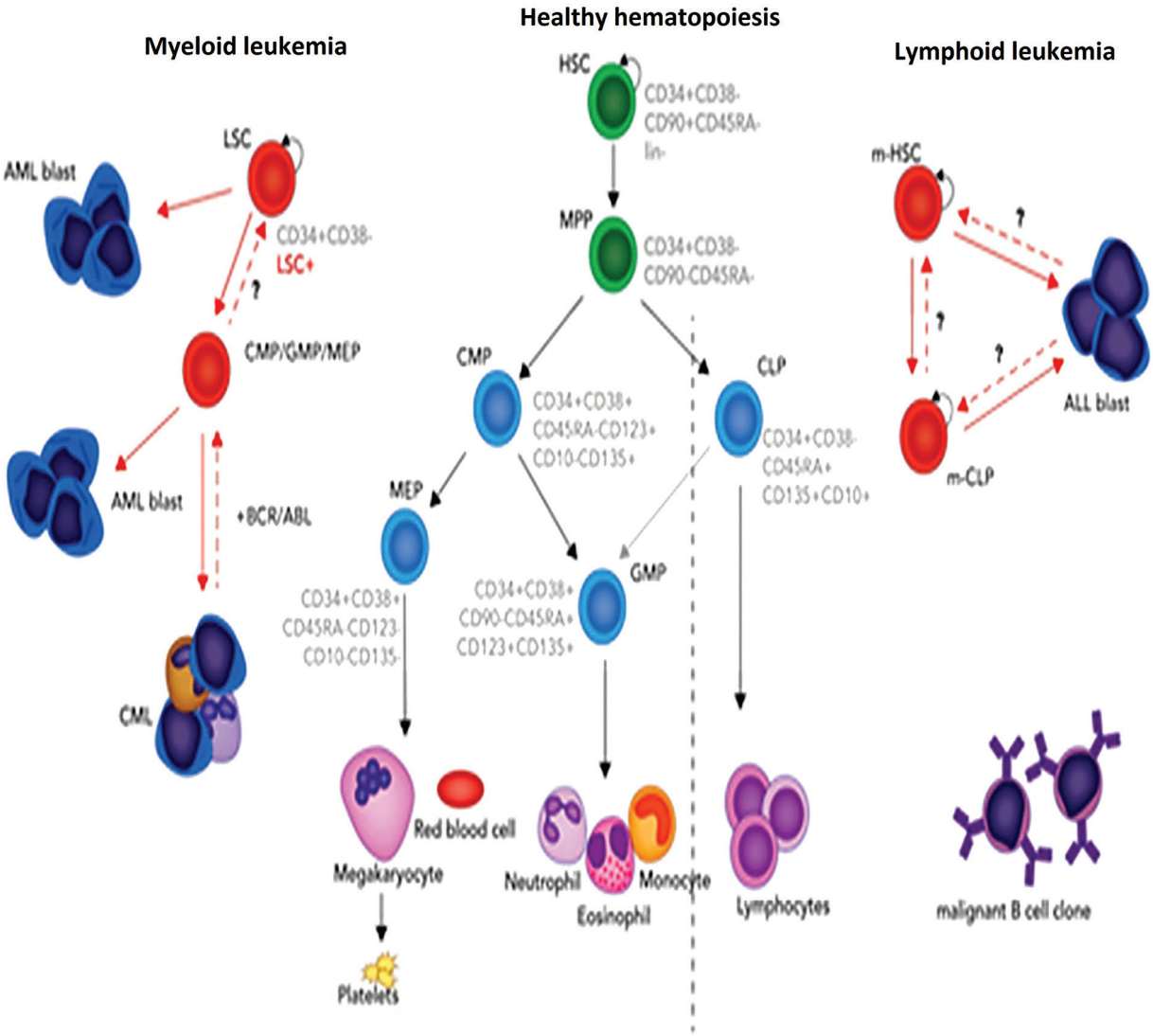

Figure 6. Hematopoiesis with hematopoietic stem cells at the forefront
Abbreviations: CLP: Common lymphoid progenitor; CMP: Common myeloid progenitor; GMP: Granulocyte–monocyte progenitor; HSC: Hematopoietic stem cell; MEP: Megakaryocyte–erythroid progenitor; MPP: Multipotent progenitor. Adapted from Barbu and Popescu.[30]

dark. Both positive and negative fluorescence controls are required. Normal residual cells or unstained cells should also be included as reference controls.

Routine flow cytometric analysis of bone marrow aspirates enables the identification of lymphocyte progenitors. Proliferated B lymphocytes are characterized by the phenotype $CD45^+$, $CD19^+$, CD90^dim/partial, $CD5^+$, $CD23^+$, $CD200^+$, $CD43^+$, sIg^dim. Lymphoid progenitors are defined by $CD34^+$, $CD38^-$, CD90^dim/$^-$, $CD45RA^+$, $CD135^+$, $CD10^+$.

Modern cytometers automatically perform compensation through integrated software. Abnormal populations (blasts) are analyzed based on CD45 receptor scatter patterns. Cells within this progenitor reservoir have the potential to generate all lymphocyte subpopulations, macrophages, and dendritic cells, and are classified as multi-lymphoid progenitors.

4.4.4. Automatic separation of multiple cell types from a single sample

Cell separation for chimerism analysis can be achieved using the EasySep™ kit. Example markers and applications include: hematopoietic progenitor cells (CD34); B progenitors ($CD34^+$, TdT^+, $CD19^+$, $CD79a^+$, $cyCD22^+$, $HLA\text{-}DR^+$, $CD10^-$, $cyIgM^-$, sIg^-); B precursors ($CD34^+$, TdT^+, $CD45^{\wedge}dim^+$, $CD19^+$, $CD79a^+$, $cyCD22^+$, $HLA\text{-}DR^+$, $CD10^{\wedge}int^+$, $cyIgM^+$, sIg^+); and mature B cells ($CD5^+$, $CD19^+$, $CD20^{+-}$, $CD23^+$).

4.4.5. Differentiation of hematopoietic stem/progenitor cells into lymphoid progenitors

$CD34^+$ hematopoietic stem/progenitor cells are seeded in untreated tissue plates coated with lymphoid expansion reagents, at protocol-specified cell densities. Medium changes are performed at regular intervals. By day 14, lymphoid-expanded cells are harvested and reseeded at 5×10^4 live cells/mL in uncoated tissue culture plates using NK differentiation medium supplemented with 1 mM UM729. A subset of cells is cryopreserved in CryoStor-CS10, while the remainder is stained with antibodies against CD5, CD7, CD43, CD45, and CD34 to monitor the progressive loss of CD34 expression during differentiation.

4.4.6. Cell analysis and instrumentation

Cell counts are performed using the Invitrogen™ Countess™ II FL Automated Cell Counter, which provides bright-field and dual-channel fluorescence analysis for monitoring viability, transfection efficiency, and protein expression. Red blood cells are lysed using a red blood cell lysis buffer, followed by two washes with phosphate-buffered saline. Cells are analyzed on a BD FACS Aria flow cytometer, and data are processed with FlowJo software, assessing green fluorescent protein (GFP) and red fluorescent protein (RFP) signals to classify edited populations: –P53^MUT: GFP^+/RFP^-; –P53-del(13p); and ATM: GFP^+/RFP^+. Following collection, edited stem cells can be reinfused into patients after cytoreduction of the bone marrow, aiming to reduce the hematopoietic burden of mutant *TP53* clones (Figure 6).

5. Conclusion

CRISPRs-based functional genomics provides a powerful platform to identify genes most affected by single-gene disruption, assess gene–gene interactions, and characterize mutation profiles associated with adverse outcomes in CLL.

CRISPR–Cas9 gene editing shows significant promise as a therapeutic strategy for *TP53*-mutant CLL by enabling precise gene correction, functional replacement, or pathway disruption. Continued improvements in delivery systems, editing efficiency, and safety monitoring will be critical for clinical translation.

Acknowledgments

None.

Funding

None.

Conflict of interest

The authors declare that they have no competing interests.

Author contributions

Conceptualization: Aurelian Udriștioiu
Data curation: Ioan-Ovidiu Gheorghe
Formal analysis: Manole Cojocaru
Investigation: Liviu Martin
Methodology: Delia Nica-Badea
Writing–original draft: Adrian Victor Tetileanu
Writing–review & editing: Aurelian Udriștioiu

Ethics approval and consent to participate

Not applicable.

Consent for publication

Not applicable.

Availability of data

Data are available from the corresponding author upon reasonable request.

References

1. Ishino Y, Shinagawa H, Makino K, Amemura M, Nakata A. Nucleotide sequence of the iap gene, responsible for

alkaline phosphatase isozyme conversion in *Escherichia coli*, and identification of the gene product. *J Bacteriol*. 1987;169(12):5429-5433.

doi: 10.1128/jb.169.12.5429-5433.1987

2. Lander ES. The heroes of CRISPR. *Cell*. 2016;164(1-2):18-28.

doi: 10.1016/j.cell.2015.12.041

3. Hille F, Charpentier E. CRISPR-Cas: Biology, mechanisms and relevance. *Philos Trans R Soc Lond B Biol Sci*. 2016;371(1707):20150496.

doi: 10.1098/rstb.2015.0496

4. Chang HH, Pannunzio NR, Adachi N, Lieber MR. Non-homologous DNA end joining and alternative pathways to double-strand break repair. *Nat Rev Mol Cell Biol*. 2017;18(8):495-506.

doi: 10.1038/nrm.2017.48.

5. Sallmyr A, Tomkinson AE. Repair of DNA double-strand breaks by mammalian alternative end-joining pathways. *J Biol Chem*. 2018;293(27):10536-10546.

doi: 10.1074/jbc.TM117.000375

6. Bhargava R, Onyango DO, Stark JM. Regulation of single-strand annealing and its role in genome maintenance. *Trends Genet*. 2016;2(9):566-575.

doi: 10.1016/j.tig.2016.06.007

7. Chen JM, Férec C, Cooper DN. Gene conversion in human genetic disease. *Genes (Basel)*. 2010;1(3):550-563.

doi: 10.3390/genes1030550

8. Verma P, Greenberg RA. Noncanonical views of homology-directed DNA repair. *Genes Dev*. 2016;30(10):1138-1154.

doi: 10.1101/gad.280545.116

9. Savic N, Ringnalda FC, Lindsay H, *et al*. Covalent linkage of the DNA repair template to the CRISPR-Cas9 nuclease enhances homology-directed repair. *Elife*. 2018;7:e33761.

doi: 10.7554/eLife.33761

10. Zaboikin M, Zaboikina T, Freter C, Srinivasakumar N. Non-homologous end joining and homology directed DNA repair frequency of double-stranded breaks introduced by genome editing reagents. *PLoS One*. 2017;12(1):e0169931.

doi: 10.1371/journal.pone.0169931

11. Qi LS, Larson MH, Gilbert LA, *et al*. Repurposing CRISPR as an RNA-guided platform for sequence-specific control of gene expression. Cell. 2013;152(5):1173-1183.

doi: 10.1016/j.cell.2013.02.022. Erratum in: Cell. 2021;184(3):844.

doi: 10.1016/j.cell.2021.01.019

12. Konermann S, Brigham MD, Trevino AE, *et al*. Genome-scale transcriptional activation by an engineered CRISPR-Cas9 complex. *Nature*. 2015;517(7536):583-588.

doi: 10.1038/nature14136

13. Polstein LR, Gersbach CA. A light-inducible CRISPR-Cas9 system for control of endogenous gene activation. *Nat Chem Biol*. 2015;11(3):198-200.

doi: 10.1038/nchembio.1753

14. Gilbert LA, Larson MH, Morsut L, *et al*. CRISPR-mediated modular RNA-guided regulation of transcription in eukaryotes. *Cell*. 2013;154(2):442-451.

doi: 10.1016/j.cell.2013.06.044

15. Zhang T, Zhu Z, Xun G, Zhao H. ScienceDirect. *Curr Opin Biomed Eng*. 2023;28:10048.

16. Tadić V, Josipović G, Zoldoš V, Vojta A. CRISPR/Cas9-based epigenome editing: An overview of dCas9-based tools with special emphasis on off-target activity. *Methods*. 2019;164-165:109-119.

doi: 10.1016/j.ymeth.2019.05.003

17. Hong Y, Lu G, Duan J Liu W, Yu Z. Comparison and optimization of CRISPR/dCas9/gRNA genome-labeling systems for live cell imaging. *Genome Biol*. 2018;19:39.

doi: 10.1186/s13059-018-1413-5

18. Schubert MS, Cedrone E, Neun B, Behlke MA, Dobrovolskaia MA. Chemical modification of CRISPR gRNAs eliminate type I interferon responses in human peripheral blood mononuclear cells. *J Cytokine Biol*. 2018;3(1):121.

doi: 10.4172/2576-3881

19. Anzalone AV, Randolph PB, Davis JR, *et al*. Search-and-replace genome editing without double-strand breaks or donor DNA. *Nature*. 2019;576(7785):149-157.

doi: 10.1038/s41586-019-1711-4

20. Zetsche B, Gootenberg JS, Abudayyeh OO, *et al*. Cpf1 is a single RNA-guided endonuclease of a class 2 CRISPR-Cas system. *Cell*. 2015;163(3):759-771.

doi: 10.1016/j.cell.2015.09.038

21. Gregg C, Ohtsuka M, Gurumurthy CB, Behlke MA. Simplified CRISPR tools for efficient genome editing and streamlined protocols for their delivery into mammalian cells and mouse zygotes. *Methods*. 2017;121-122:16-28.

doi: 10.1016/j.ymeth.2017.03.021

22. Miura H, Gurumurthy CB, Sato T, Sato M, Ohtsuka M. CRISPR/Cas9-based generation of knockdown mice by intronic insertion of artificial microRNA using longer single-stranded DNA. *Sci Rep*. 2015;5:12799.

doi: 10.1038/srep12799

23. Yoshimi K, Kunihiro Y, Kaneko T, Nagahora H, Voigt B, Mashimo T. ssODN-mediated knock-in with CRISPR-Cas for large genomic regions in zygotes. *Nat Commun*. 2016;7:10431.

doi: 10.1038/ncomms10431

24. Crosetto N, Mitra A, Silva MJ, *et al*. Nucleotide-resolution DNA double-strand break mapping by next-generation sequencing. *Nat Methods*. 2013;10(4):361-365.

    doi: 10.1038/nmeth.2408

25. Kim D, Bae S, Park J, *et al*. Digenome-seq: Genome-wide profiling of CRISPR-Cas9 off-target effects in human cells. *Nat Methods*. 2015;12(3):237-43, 1 p following 243.

    doi: 10.1038/nmeth.3284

26. Tsai SQ, Nguyen NT, Malagon-Lopez J, Topkar VV, Aryee MJ, Joung JK. CIRCLE-seq: A highly sensitive *in vitro* screen for genome-wide CRISPR-Cas9 nuclease off-targets. *Nat Methods*. 2017;14(6):607-614.

    doi: 10.1038/nmeth.4278

27. Cameron P, Fuller CK, Donohoue PD, *et al*. Mapping the genomic landscape of CRISPR-Cas9 cleavage. *Nat Methods*. 2017;14(6):600-606.

    doi: 10.1038/nmeth.4284

28. Tsai SQ, Zheng Z, Nguyen NT, *et al*. GUIDE-seq enables genome-wide profiling of off-target cleavage by CRISPR-Cas nucleases. *Nat Biotechnol*. 2015;33(2):187-197.

    doi: 10.1038/nbt.3117

29. Wienert B, Wyman SK, Richardson CD, *et al*. Unbiased detection of CRISPR off-targets *in vivo* using DISCOVER-Seq. *Science*. 2019;A364(6437):286-289.

    doi: 10.1126/science.aav9023

30. Barbu D, Popescu DM. Immunophenotypic diagnosis in images. In: *Clinical Hematology Laboratory Notebooks*. Bucharest: Medical Publishing House; 2018.

31. Udristioiu A, Gheorghe IG, Nica-Badea D. *Book "Isoform p53 Protein's Major Role in the Pathophysiology of Malignant Hematologic Diseases*. Ch. 2. Cambridge, UK: Cambridge Scholars Publishing; 2024.

32. Lefter M, Vis JK, Vermaat M, den Dunnen JT, Taschner PE, Laros JFJ. Mutalyzer 2: Next generation HGVS nomenclature checker. *Bioinformatics*. 2021;37:2811-28117.

    doi: 10.1093/bioinformatics/btab051